

# Thermal Shock Induced by a 24 GeV Proton Beam in the Test Windows of the Muon Collider Experiment E951 – Test Results and Theoretical Predictions

N. Simos<sup>1</sup>, H. Kirk<sup>1</sup>, K. McDonald<sup>2</sup>, M. Cates<sup>3</sup>, J. Tsai<sup>3</sup>, D. Beshears<sup>3</sup>, B. Riemer<sup>3</sup>, C. Fincock<sup>1</sup>,  
R. Prigl<sup>1</sup>, K. Brown<sup>1</sup>, S. Kahn<sup>1</sup> and H. Ludewig<sup>1</sup>

<sup>1</sup>Brookhaven National Laboratory, Upton, NY 11973, USA; simos@bnl.gov

<sup>2</sup>Princeton University, USA

<sup>3</sup>Oak Ridge National Laboratory, USA

## Abstract

The need for intense muon beams for muon colliders and neutrino factories has led to a concept of a high performance target station in which a 1-4 MW proton beam of 6-24 GeV impinges on a target inside a high field solenoid channel. While novel technical issues exist regarding the survivability of the target itself, the need to pass the tightly focused proton beam through beam windows poses additional concerns. In this paper, issues associated with the interaction of a proton beam with window structures designed for the muon targetry experiment E951 at BNL are explored. Specifically, a 24 GeV proton beam up to  $16 \times 10^{12}$  per pulse and a pulse length of approximately 100 ns is expected to be tightly focused (to 0.5 mm rms one sigma radius) on an experimental target. Such beam will induce very high thermal, quasi-static and shock stresses in the window structure that exceed the strength of most common materials. In this effort, a detailed assessment of the thermal/shock response of beam windows is attempted with a goal of identifying the best window material candidate. Further, experimental strain results and comparison with the predicted values are presented and discussed.

## 1. INTRODUCTION

A muon collider or a neutrino factory based on a muon storage ring requires a tightly focused, high intensity beam on target. Specifically, up to 16 TP per pulse (1 TP =  $10^{12}$  protons) of a 24 GeV proton beam need to be delivered on a target, with a pulse length of a few microseconds and a beam spot of 0.5 mm radius. While a mercury jet is the primary target consideration (high-Z material and more efficient in producing pions of both signs), other options using graphite as target material (low-Z and better in avoiding the absorption of produced pions) are also being explored.

While a number of other studies deal with the pion production [1,2,3], this study focuses on the thermo-mechanical response of materials, especially beam windows when they interact with the intense proton beam. Prior to entering the target space, the proton beam must go through a beam window structure. From the required muon collider beam parameters it may be

concluded that very few, if any, materials will be able to survive the thermal shock that will be induced. While in the actual muon collider target the beam window location can be optimized based on the beta function and achieve a bigger spot, the E951 experiment at BNL will require for the beam window to be close to the target where the beam focuses down to its smaller spot. In order to select the right window material that will survive under such conditions, an extensive effort was undertaken to evaluate different materials that show promise based on their mechanical strength. The effort consisted of the calculation of energy deposition on the different materials using the hadron interaction code MARS [10], the transient thermal analysis resulting from the deposited energy and finally the thermal stress analysis that included the generation and propagation of stress waves. The thermal response of the window structure and the subsequent stress wave generation and propagation are computed using the finite element analysis procedures of the ANSYS [11] code.

Experiment E951 has been approved for running at the Brookhaven Alternating Gradient Synchrotron (AGS). Figure 1 depicts the layout of the A3 beam line near the target station that has been configured for the transport of primary 24 GeV protons extracted from the AGS. All targets are mounted inside a stainless steel vessel preventing any dispersal of activated fragments that can potentially be ejected from the tested target. Figure 2 represents the beam spot size in the two planes at the end of the A3 line that may be achieved through fine-tuning of the various quadrupoles. Figure 2 shows that a spot size of 0.5mm radius is achievable.

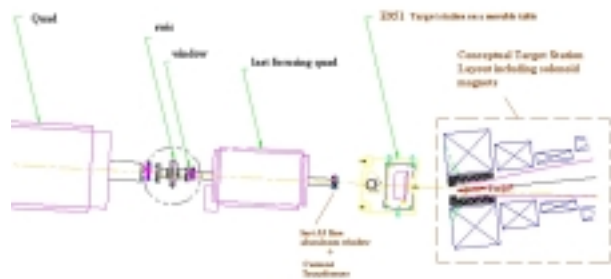


Figure 1. AGS A3 Line layout at E951 target station.

## 2. THERMOELASTIC THEORY

Consider a thin window structure of radius  $R$  and thickness  $h$  intercepting an energetic, focused proton beam of Gaussian profile. Energy is deposited in the material with radial symmetry about the window center while some variation of energy deposited is expected to be present, no matter how thin the window, through the thickness  $h$ .

In evaluating the thermoelastic equation of motion in the beam window it is assumed that the thermal expansion is isotropic and the effects of heat conduction on the dynamics are neglected. Further, as first approximation, no attenuation of the acoustic pulse is accounted for even though some fraction of the energy is dissipated in the material. It is also assumed throughout that the energy deposited in the window material is immediately converted to thermal energy. As noted in [6] this is a very good approximation given that the acoustic relaxation time is of the order of ns whereas “thermalization” times, at least in metals are of the order of  $10^{-11}$  secs.

Based on the above considerations, the issue to address is how does a thin window structure respond as it intercepts a fast and intense proton pulse. While “thermalization” is assumed to take place instantly, thus generating a quasi-static state of stress in the affected zone, the acoustic relaxation time still plays a role in defining both the generation and the level of thermal shock stresses. Specifically, the amplitude of the stress waves emanating from the “heated” zone depends on the relation between the rate of energy deposition (pulse length) and the acoustic relaxation time (time required for an acoustic wave to traverse the region of energy deposition). If the time of energy deposition is smaller than the acoustic relaxation, the amplitude of the stress wave will be maximal. If the opposite is true, then the stress amplitude will be reduced based on the ratio of the two characteristic times.

While the above considerations define the response of the thin window in the radial sense of stress wave generation and propagation, the most important consideration in assessing its survivability is the thermoelastic response through the window thickness. As the affected zone is thermalized in the cylindrical volume between the two surfaces, stress waves initiate at each of the surfaces and travel toward the opposite surface. The governing principle is basically a 1-D response similar to the response of a heated 1-D rod with free edges.

To demonstrate the severity of the beam-window interaction under such tight focusing, the thermal stress induced in a 10-mil thick stainless steel window by the beam of the required parameters (24 GeV, 16 TP, 0.5 mm rms sigma and 100 ns pulse length) is estimated. Figure 3 shows the temperature rise in the stainless steel

window as a result of a single pulse. The peak von Mises stresses in the window material, occurring at beam center and mid-thickness, approaches 2500 MPa which is more than twice the yield and ultimate strength of the material. According to this prediction such window will not be able to survive a single pulse let alone multiple pulses. Shown in Figure 4 is the “ringing” regime that follows the energy deposition. The peak von Mises stress occurs within the window thickness some time between the initiation of the pulse and the time required for the sound to traverse the thickness for the first time.

Figure 5 graphically demonstrates the response of the heated zone by capturing the propagation and reflection of elastic waves through the thickness and out of the zone in a series of snap shots. Since energy is moving out of the region in the radial direction, the amplitude of the stress “ringing” through the thickness reduces in time. The impact on the window material, however, could be dramatic since a significant number of stress cycles of considerable amplitude can accumulate following a proton pulse. Figure 6 is a verification of the expected wave propagation through the thickness based on simulation of the process.

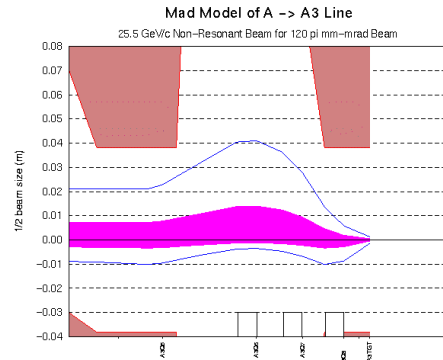


Figure 2. Proton beam focusing at AGS A3 line for experiment E951

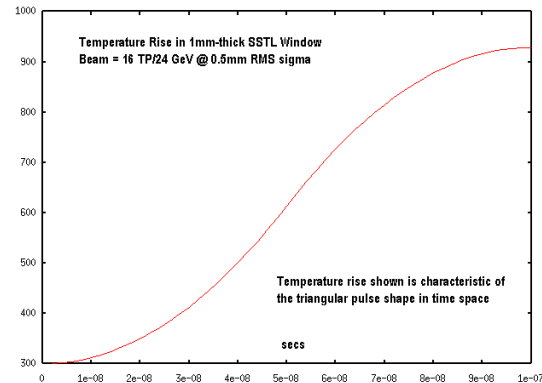
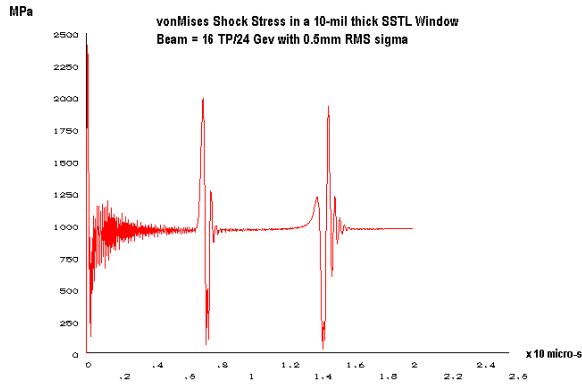
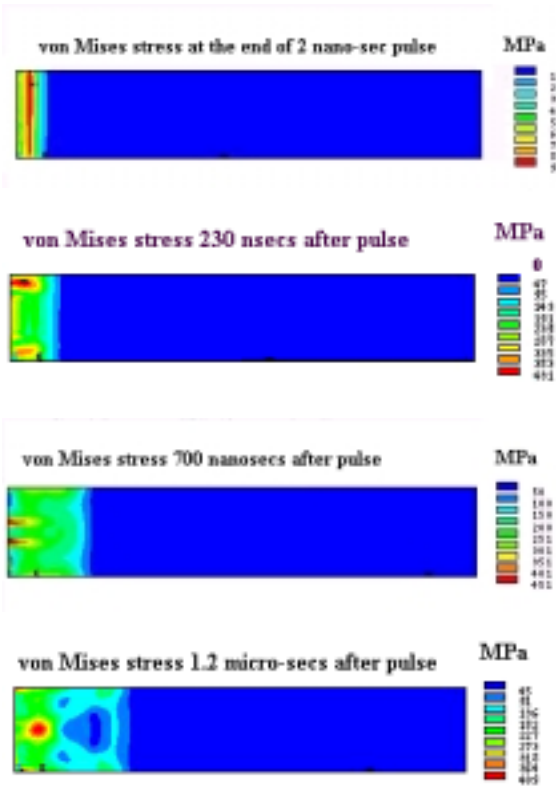


Figure 3. Temperature rise from a single pulse in a stainless steel window.



**Figure 4.** von Mises stress in a stainless steel window intercepting a 24 GeV proton beam with 16 TP intensity and 0.5 mm radius beam spot



**Figure 5:** von Mises stress wave propagation following a proton pulse on an Inconel-718 window

Initial estimates of energy deposition in various materials for a 24 GeV proton beam, 16 TP intensity, a beam spot down to 0.5 mm radius and a pulse length of approximately 100 ns painted a very bleak picture for most commonly used materials for beam windows. An additional concern, in bringing beam down the AGS A3 line, was the ability of existing aluminum windows to survive even though there were expected to see a larger spot (based on the beta function of the beam). Given the severity of the problem, an experimental set-up to study

the response of window materials as part of the E951 muon targetry experiment was introduced. Four (4) different window materials were selected for testing in the beam line at AGS. Three of the materials, Inconel-718, Havar and Titanium alloy, showed promise of surviving the proton beam pulses. Their selection was based on material properties and extensive thermal shock predictions. Figure 7 shows von Mises stresses generated in a titanium alloy (6% Al – 6% V). Under the required parameters of 24 GeV, 16 TP intensity and 0.5-mm rms spot, the stresses are below yield, thus making it a favorable candidate. Figure 8 presents similar results in a Havar window and shows that under such beam parameters the peak stresses are approaching the yield stress limit. Figure 9 addresses the level of stress anticipated in a thin aluminum window.

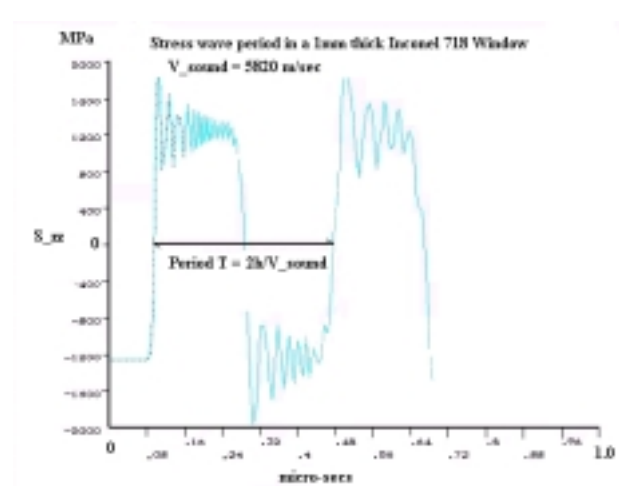


**Figure 6:** Verification of "through-thickness" wave propagation using transient finite element analysis.

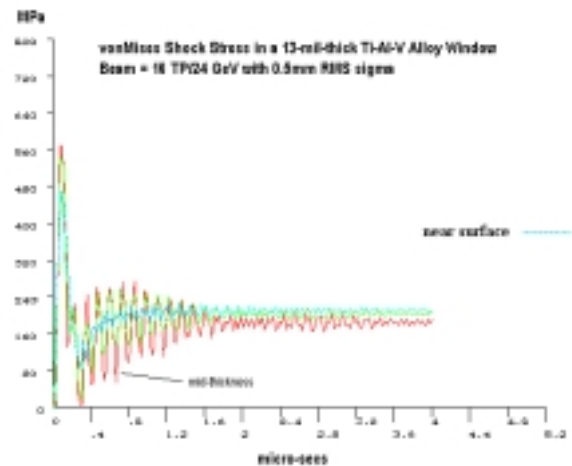


**Figure 7:** von Mises shock stresses in a Titanium alloy window. Minimum yield stress = 931 MPa

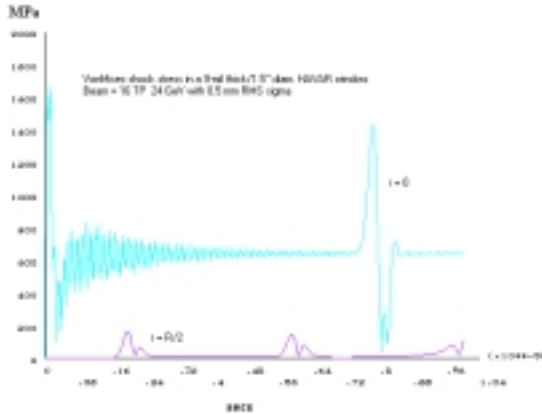


**Figure 8: von Mises shock stresses in a 9-mil thick Havar window from a 24 GeV, 16 TP and 0.5 mm radius beam. Material yield stress = 1940 MPa**

The fourth material selected is Aluminum (3000-Series). Based on the theoretical predictions, this window material could fail even if 6 TP are delivered on target. Given that at initial stages of E951 6 TP beam is more likely to be delivered and because of the proximity of this window material to the failure condition, experimental data associated with this material and its potential failure, would be very useful in benchmarking failure prediction.

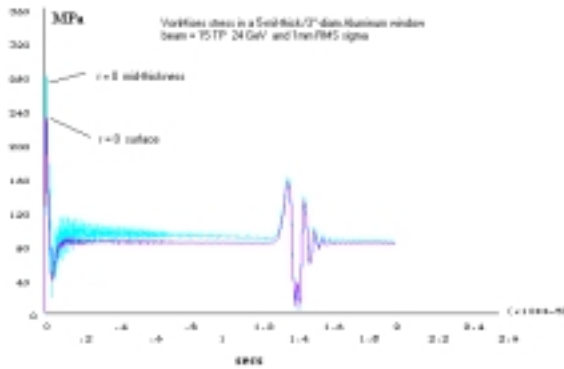


**Figure 9: Shock von Mises stresses in an aluminum window similar to beam windows used in the AGS A3 line induced by a 24 GeV proton beam of intensity 16 TP and 1 mm radius beam spot**

Since the calculations show that the window thickness, in conjunction with the material acoustic velocity and the pulse structure and duration, has a dramatic effect on the peak stresses generated in the material, two (2) thicknesses (1-mm and 6-mm) of the Inconel-718 material were selected for study.

## 2. E951 EXPERIMENT

Figure 10 depicts the layout of the window test experiment. There are two parallel beam lines within the target enclosure. It all rests on a moving table such that both lines can be exposed to the proton beam. Shown in Figure 10 and in one of the lines is a set of double windows with vacuum in the space between the two plates. Each window is made of one of the selected experiment materials. The main goal is to make a quantitative assessment of window failure when it intercepts the proton beam. In other words, any loss of vacuum, which is continuously monitored, in the space between the double windows will indicate mechanical failure. Along the second beam line a set of single windows instrumented with fiber-optic strain gauges are placed. The details of the set-up and of the acquisition system are given in more detail in the following subsection.

### 2.1 Strain Measurement Set-Up

The goal of the strain experiment is to capture the radial strain at a specified distance from the beam spot location. While the governing shock stress in determining the safety of the window material is the von Mises stress at the center of the spot and through the material thickness, there is no measurable quantity in that orientation. However, by predicting the radial strain at a safe distance from the beam (minimize the radiation damage on the strain gauges), the whole stress tensor can be estimated. Figure 11 depicts the arrangement of four (4) fiber-optic strain gauges that were placed on the front surface of each of the tested windows. The strain gauges were designed around an interferometer and made by FISO Technologies Inc. The basic active element (cavity) consists of two mirrors facing each other. The acquired signal goes through custom-made filtering and at the end of the process a 500 kHz strain signal is deduced.

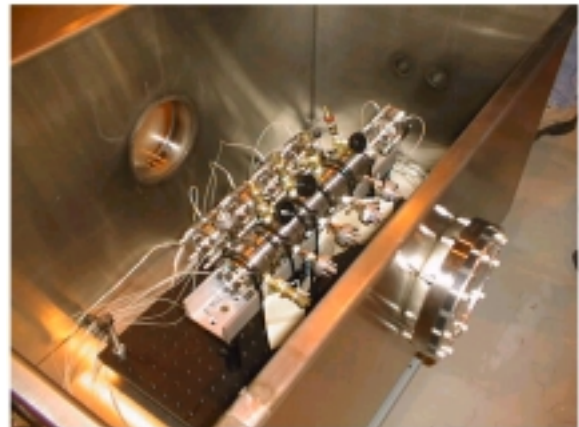


**Figure 10: Window test set-up at E951 experiment**

The wavelength of the shock front (uncorrupted by reflections from a less than ideal window boundary) and the ability of recording system to capture it is vital to the analysis of strain amplitude and time structure.

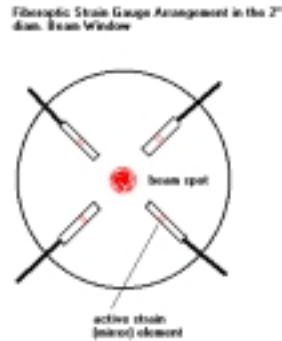


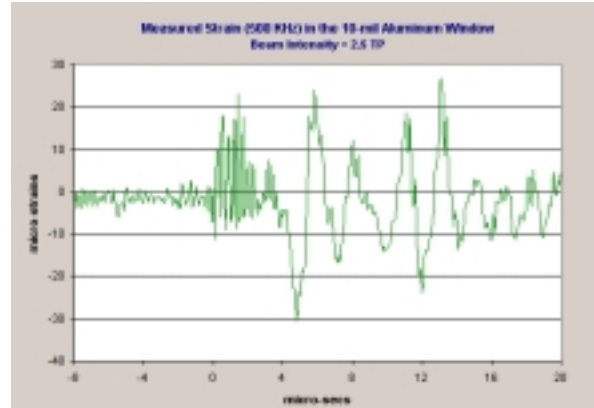
**Figure 11: Schematic arrangement of the fiber-optic strain gauges in the test windows**

## 2.2 Strain Measurements

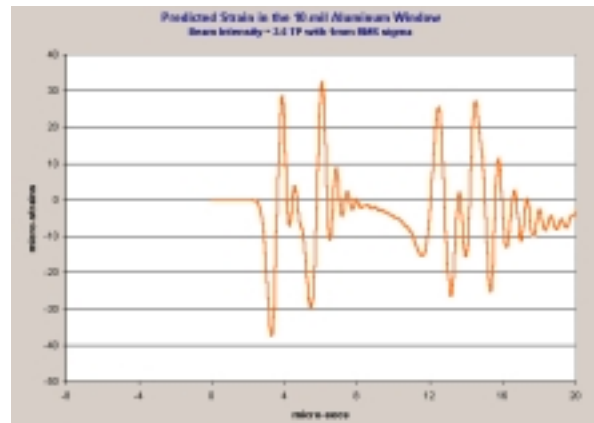
During the window tests of the E951 experiment a beam intensity of approximately 2.5 TP was delivered on target while the beam spot was approximately 1mm radius. The beam spot closely fit an ellipse rather than the circle that was assumed in the theoretical predictions. While the combination of beam intensity and spot was far from being critical for any of the windows, strain measurements that can be used to verify the predictions have been generated. Shown in Fig. 12 is the radial strain in one of the four gauges of the 10-mil aluminum window. The very first part of the record is the noise in the fiber-optic system. The arrival of the proton beam is indicated by the high frequency noise corruption of the signal. The arrival of the compressive wave at the active element of the gauge (approximately at 0.5-inch from center) is shown by the first dip. What follows is the arrival of the tensile wave phase at precisely the time that is expected.

Following the rapid thermalization of the affected material (within the beam spot) two waves are generated at the edge of the heated zone. One travels outward as a compressive wave and arrives at the strain gauge first (dip). The second wave travels toward the center of the beam spot as compressive, reflects at the center by changing sign, and travels outward as a tensile wave. The remaining cycles represent reflections at the edge of the window and its center.

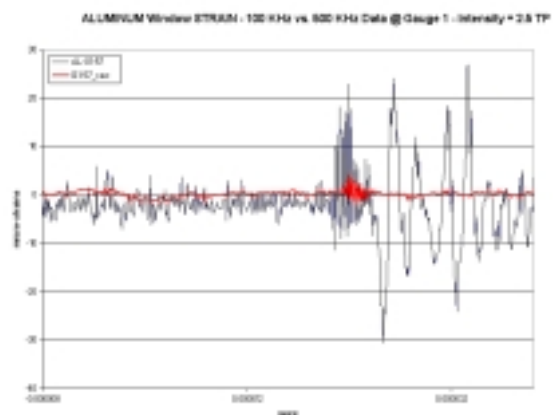
Figure 13 depicts the calculated strains for the same beam parameters but with a “true” round Gaussian profile. The agreement between experiment and theory is very good both in terms of amplitude and time structure.



**Figure 12: Radial strain measured in the 10-mil aluminum window and induced by a 24 GeV, 2.5 TP and approximately 1mm rms one sigma radius beam**



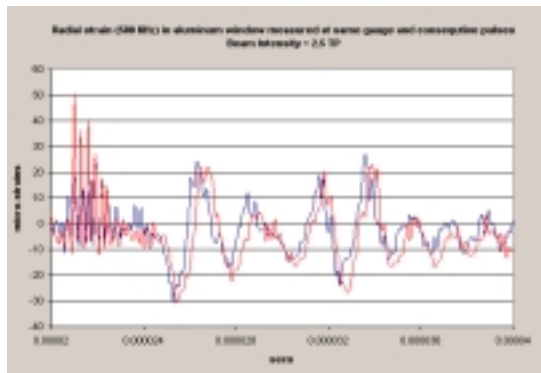
**Figure 13: Predicted strains (ANSYS) in the 10 mil aluminum window for 2.5 TP and 1mm radius beam**



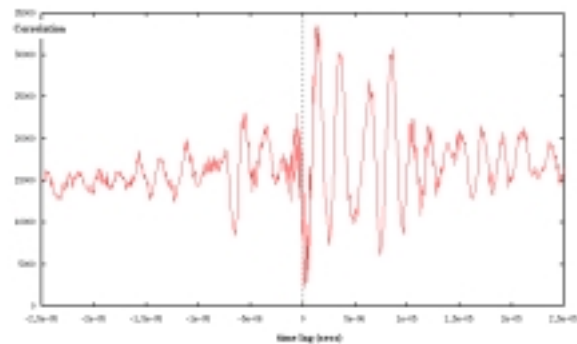
**Figure 14: Comparison of measured strains between a 100 kHz and a 500 kHz processed strain signal in the vicinity of the arrival of the initial shock wave at mid-radius of the aluminum window**

Figure 14 depicts the recorded strain of the same gauge as seen from two bandwidths of the acquisition system. The strain record shows the arrival of the initial shock wave and some reflections of the pulse between the edge and the center of the window disk. Based on the AGS pulse structure, spot size and pulse length, it was assessed that the 100 kHz bandwidth was insufficient to record the stress pulse arrival at the strain gauge location. Indeed, Figure 14 clearly demonstrates that no signal was recorded by the acquisition system operating at this bandwidth. Not shown here is the complete record (up to 0.1 sec) which shows that overall response of the window dominated by lower frequencies is captured by both bandwidths.

Figure 15 shows the strain measurements at the same gauge in two back-to-back pulses with approximately the same beam intensity. The duplication of the response is a sign of stability in the measurements. However, it should be noted that fiberoptic strain signal is very sensitive to the beam arrival and the ensuing flux of photons (shown as high frequency bunch at the start of the record and sharp peaks in the transient response). A filtering effort is under way to “clean” the records from the inherent and induced noise.



**Figure 15: Strain measured in aluminum window in back-to-back pulses of similar intensity**



**Figure 16: Cross Correlation of signals recorded by different gauges of the same window to assess the position of the pulse relative to the strain gauges.**

An additional source of discrepancy is the actual position of the beam with regard to the four gauges. A beam shift toward one of them will alter the strain measurements by inducing higher strains in the closest gauge. To estimate the “true” position of the beam, a cross-correlation process (typical results shown in Figure 16) of the gauge signals has been introduced that, in first order, indicates the relative arrival of the signal. In Figures 17 & 18 the measured and predicted strains in the 1mm-thick Inconel-718 window are shown. It should be noted that based on the “preliminary” analysis and comparison of experimental to theoretical results, it has been observed that the thicker the window gets the higher the deviation between the two.

In Figure 19 the strain recorded in the 6mm-thick window are shown. As expected, the “thickness” effect becomes more prominent in that there is presence of surface waves that have been enabled to form and propagate as well as delayed reflections from the opposite surfaces. Figure 20 depicts the theoretical predictions in the same window but with a Gaussian spot at the center of the window. It is evident that general characteristics of the response are predicted quite well. Lastly, in Figure 21 the recorded strains from back-to-back pulses are shown for the thin Havar window demonstrating the stability of the acquisition system.

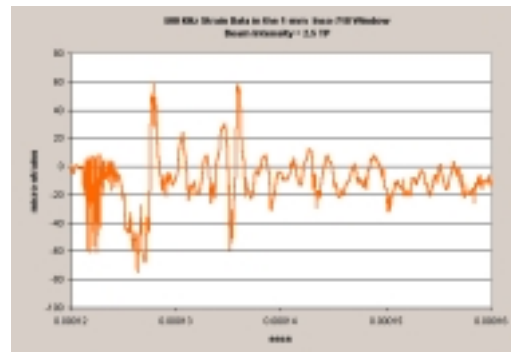


**Figure 17: Recorded strain in 1mm Inconel window**

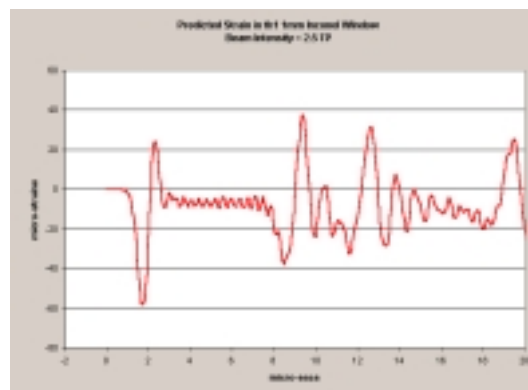


**Figure 18: Predicted strain in 1mm Inconel window**

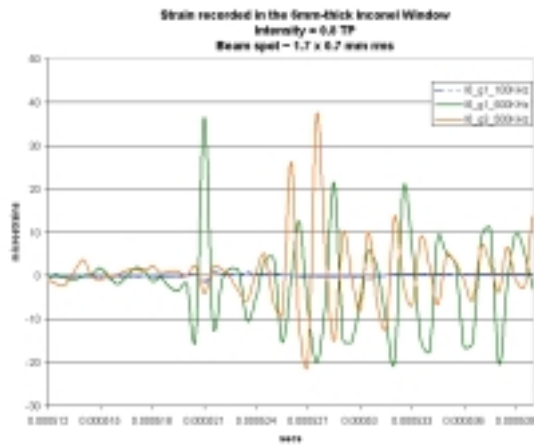


**Figure 19: Recorded strain in a 6-mm Inconel window by two strain gauges 180 deg apart. Also shown is the recorded signal by the 100 kHz bandwidth sensor.**

### 3. SUMMARY

As part of the R&D program of the Neutrino Factory and Muon Collider Collaboration on targetry, BNL experiment E951 has been conducted in the spring of 2001. The broad goal of E951 was to provide a facility that can test all the major components of a liquid or solid targets in intense proton pulses and in a 20 Tesla magnetic field. The completed first phase of E951 focused on the interaction of intense proton pulses with targets and beam windows in zero magnetic field.

This first phase of the targetry experiment E951 provided the opportunity to test, in addition to targets, window structures that are integral part of any target system and normally experience similar shock conditions. What has been deduced, so far, from the experimental/theoretical results are the following:

- Good agreement is seen in strains of thin windows. This implies that the energy deposition estimated by the neutronic code calculations agrees with the energy left in the material by the beam. It should be noted that in this first phase of data post-processing and comparison, no material damping has been introduced in the theoretical predictions. Subsequent analyses with energy dissipation considerations would help the agreement both in terms of amplitude and pulse shape and dispersion even further
- Because of the lower than anticipated intensity and larger beam spot, the failure conditions for the weakest window (aluminum) were never approached

- The thicker the window, the more difficult it is to predict amplitudes and structure of the signal due to multiple wave phases and reflection
- Given the nature of shock waves in the materials, a further increase in the measuring system bandwidth is desirable

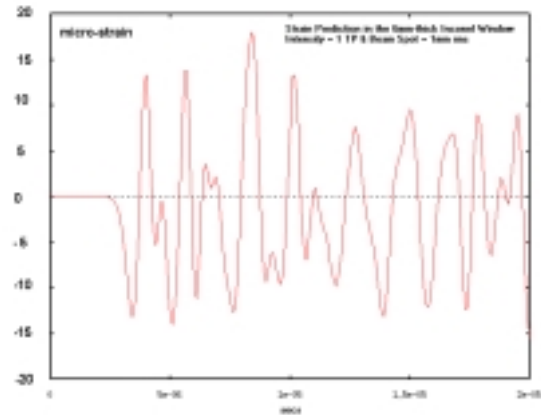


**Figure 20: Predicted strains in the 6mm-thick Inconel 718 window**

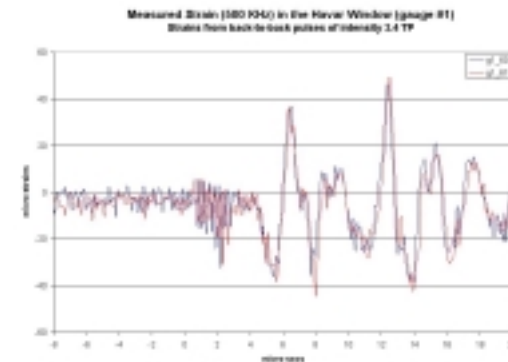


**Figure 21: Recorded strains in back-to-back pulses in an 11mil-thick Havar window**

### ACKNOWLEDGMENTS

Work performed under the auspices of the U.S. Dept. of Energy.

### REFERENCES

[ 1 ] M. Zisman, Status of Neutrino Factory and Muon Collider R&D, PAC2001, WOAB008, 2001

[ 2 ] S. Osaki et al., eds., Feasibility Study-II of a Muon Based Neutrino Source, 2001, <http://www.cap.bnl.gov/mumu/studyii/FS2-report.html>

- [ 3 ] H. Kirk et al., "Target Studies with BNL E951 at AGS," PAC2001, TPAH137, 2001
- [ 4 ] K. Brown, et al., "First Beam Tests of the Muon Collider Target Test Beam Line at the AGS," PAC2001, TPAH129,2001
- [ 5 ] N. Simos, et al., "Thermal Shock Analysis of Windows Interacting with Energetic, Focused Beam of the BNL Muon Target Experiment," PAC2001, TPAH085,2001
- [ 6 ] R.B. Oswald, et al., "One-Dimensional Thermoelastic Response of Solids to Pulsed Energy Deposition," Journal of Applied Physics, Vol. 42, No. 9, pp. 3463-3473, 1971
- [ 7 ] D. Burgreen, "Thermoelastic Dynamics of Rods, Thin Shells and Solid Spheres", Nucl. Sc. And Eng., 12, 203-217, 1962
- [ 8 ] P. Sievers, "Elastic Stress Waves in Matter due to Rapid Heating by Intense High-Energy Particle Beam," LAB.II/BT/74-2, CERN, 1974
- [ 9 ] H. Conrad, "On Elastic Stress Waves in Targets", Institut fur Festkorperforschung, 1994
- [ 10 ] N.V. Mokhov, "The MARS Code System User Guide, Version 13 (95)", 1995
- [ 11 ] ANSYS Engineering Analysis of Systems, Swanson Analysis Systems Inc., 1999